Published in final edited form as:
Glia. 2010 August 15; 58(11): 1267–1281. doi:10.1002/glia.21001.

Altered levels and distribution of APP and its processing enzymes in Niemann-Pick Type C1-deficient mouse brains

A. Kodam[1,*], **M. Maulik**[2,*], **K. Peake**[2], **A. Amritraj**[1], **K.S. Vetrivel**[3], **G. Thinakaran**[3], **J.E. Vance**[2], and **S. Kar**[1,2]

[1]Department of Psychiatry, Centre for Prions and Protein Folding Diseases, University of Alberta, Edmonton, Alberta, Canada T6G 2M8

[2]Department of Medicine, Centre for Prions and Protein Folding Diseases, University of Alberta, Edmonton, Alberta, Canada T6G 2M8

[3]Departments of Neurobiology, Neurology and Pathology, The University of Chicago, Chicago, IL 60637, USA

Abstract

Niemann-Pick type C (NPC) disease is an autosomal recessive neurodegenerative disorder characterized by intracellular accumulation of cholesterol and glycosphingolipids in many tissues including the brain. The disease is caused by mutations of either *NPC1* or *NPC2* gene and is accompanied by a severe loss of neurons in the cerebellum, but not in the hippocampus. NPC pathology exhibits some similarities with Alzheimer's disease, including increased levels of amyloid β (Aβ)-related peptides in vulnerable brain regions, but very little is known about the expression of amyloid precursor protein (APP) or APP secretases in NPC disease. In the present study, we evaluated age-related alterations in the level/distribution of APP and its processing enzymes, β- and γ-secretases, in the hippocampus and cerebellum of *Npc1*$^{-/-}$ mice, a well-established model of NPC pathology. Our results show that levels and expression of APP and β-secretase are elevated in the cerebellum prior to changes in the hippocampus, whereas γ-secretase components are enhanced in both brain regions at the same time in *Npc1*$^{-/-}$ mice. Interestingly, a subset of reactive astrocytes in *Npc1*$^{-/-}$ mouse brains expresses high levels of APP as well as β- and γ-secretase components. Additionally, the activity of β-secretase is enhanced in both the hippocampus and cerebellum of *Npc1*$^{-/-}$ mice at all ages, while the level of C-terminal APP fragments is increased in the cerebellum of 10-week-old *Npc1*$^{-/-}$ mice. These results, taken together, suggest that increased level and processing of APP may be associated with the development of pathology and/or degenerative events observed in *Npc1*$^{-/-}$ mouse brains.

Keywords

Apoptosis; β-amyloid peptide; β-secretase; Cholesterol; γ-secretase; Neurodegeneration; Reactive astrocytes

Address correspondence to: Satyabrata Kar, Ph.D., Centre for Prions and Protein Folding Diseases, Departments of Medicine (Neurology) and Psychiatry, University of Alberta, Edmonton, Alberta, Canada T6G 2M8, Tel. no: (780) 492 9357; Fax no: (780) 492 9352, skar@ualberta.ca.
*These authors contributed equally to this study.

INTRODUCTION

Niemann-Pick type C (NPC) disease is an autosomal recessive neurovisceral disorder characterized by abnormal accumulation of unesterified cholesterol and glycosphingolipids within the endosomal-lysosomal (EL) system in a number of tissues including the brain. These defects in cholesterol sequestration trigger abnormal liver and spleen function as well as widespread neurological deficits such as ataxia, dystonia, seizures and dementia that eventually lead to premature death (Mukerjee and Maxfield, 2004; Pacheco and Lieberman, 2008; Pentchev et al., 1995; Vance, 2006; Vanier and Suzuki, 1998). In the majority of cases, NPC disease is caused by loss-of-function mutations in the *NPC1* gene, which encodes a transmembrane glycoprotein implicated in the intracellular transport of cholesterol (Carstea et al., 1997; Walkley and Suzuki, 2004). Interestingly, phenotypes similar to human NPC disease are also seen in Balb/cNctr-npc$^{N/N}$ mice which due to a spontaneous deletion/ insertion mutation in the *Npc1* gene do not express Npc1 protein (*Npc1*$^{-/-}$). These *Npc1*$^{-/-}$ mice are usually asymptomatic at birth but gradually develop tremor and ataxia and die prematurely between 10–12 weeks of age (Karten et al., 2003; Li et al., 2005; Loftus et al., 1997; Paul et al., 2004). At the cellular level, *Npc1*$^{-/-}$ mice show accumulation of unesterified cholesterol in the EL system, activation of microglia and astrocytes as well as loss of the myelin sheath throughout the central nervous system, phenotypes that are similar to those observed in human NPC disease. Progressive loss of neurons is also evident in the prefrontal cortex, thalamus, brainstem and cerebellum, but not much in the hippocampus (Baudry et al., 2003; German et al., 2001; Sarna et al., 2003). Although abnormal accumulation of cholesterol has been implicated in the loss of neurons in a variety of experimental paradigms, very little is currently known about the cellular changes that are associated with the degeneration of select populations of neurons in *Npc1*$^{-/-}$ mouse brains.

A number of earlier studies have shown that altered level/distribution of cholesterol can influence the sorting/processing of a variety of proteins including amyloid precursor protein (APP), which serves as the precursor for the amyloidogenic amyloid β (Aβ)-related peptides (Burns et al., 2003; Davis, 2008; Puglielli et al., 2003; Reid et al., 2007). The Aβ peptides have been implicated in the degeneration of synapses and neurons in Alzheimer's disease (AD) pathology, which exhibits some similarities with NPC disease (St George-Hyslop and Petit, 2005; Kar et al., 2004; Koh and Cheung, 2006; Nixon, 2004; Selkoe, 2008). Under normal conditions, mature APP is proteolytically processed by non-amyloidogenic α-secretase or amyloidogenic β-secretase pathways. The α-secretase cleaves APP within the Aβ domain, yielding soluble N-terminal APPα and a 10kD C-terminal fragment (α-CTF) that can be further processed by γ-secretase to generate $A\beta_{17–40}$/$A\beta_{17–42}$ fragments. The β-secretase, on the other hand, cleaves APP to generate soluble APPβ and an Aβ-containing C-terminal fragment (β-CTF), which is subsequently processed *via* γ-secretase to yield full-length $A\beta_{1–40}$/$A\beta_{1–42}$ peptides (Clippingdale et al., 2001; Thinakaran and Koo, 2008). While β-secretase is an aspartyl protease called β-site APP cleaving enzyme (BACE1), γ-secretase comprises the aspartyl protease presenilin 1 or 2 (PS1/PS2) and three cofactors, i.e., nicastrin, presenilin enhancer 2 (PEN2) and anterior pharynx defective 1 (APH1) (Cole and Vassar, 2008; Steiner et al, 2008).

There is evidence that elevated cholesterol level/accumulation can enhance generation of Aβ-related peptides, whereas inhibition of cholesterol synthesis may lower Aβ levels (Fassbender et al., 2001; Frears et al., 1999; Puglielli et al., 2003; Simons et al., 1998; Yamazaki et al., 2001). Some recent studies have indicated that NPC pathology may be associated with an altered distribution of PS1, which can influence processing of APP leading to increased levels of Aβ peptide (Burns et al., 2003). This finding is partly supported by the observation that intracellular accumulation of $A\beta_{1–42}$ and β-CTF is

increased in vulnerable regions of the NPC brain (Jin et al., 2004; Yamazaki et al., 2001). Although these results suggest a role for Aβ in the development/progression of NPC pathology, at present, very little is known about the cellular origin or its association, if any, to the neuronal vulnerability observed in NPC brains. To address this issue, we evaluated age-related changes in the levels and distribution of APP and its processing enzyme BACE1, as well as four components of the γ-secretase complex, in the hippocampus and cerebellum of *Npc1*$^{-/-}$ and control mice. In parallel, we measured the activity of α- and β-secretases as well as the levels of α- and β-CTFs to establish whether APP processing in *Npc1*$^{-/-}$ mice is altered, leading to increased production of Aβ peptides.

MATERIALS AND METHODS

Materials

Polyacrylamide (4–20%) electrophoresis gels were purchased from Invitrogen (Burlington, ON, Canada) and the enhanced chemiluminescence kit was obtained from Amersham (Mississauga, ON, Canada). The characterization and specificity of the polyclonal anti-nicastrin, anti-PS1 and anti-PEN2 antisera used in this study have been described previously (Kodam et al., 2008; Vetrivel et al., 2004). The well characterized polyclonal APP C-terminus antibodies used in this study include CT15 (provided by Dr. E. Koo, University of California, San Diego, CA), 369 (provided by Dr. S. Gandy, Mount Sinai School of Medicine, New York, NY) and CTM1 (Vetrivel et al., 2009). Polyclonal anti-myelin associated glycoprotein (MAG) was obtained from Santa Cruz Biotechnology (San Diego, CA) and anti-BACE1, anti-APH1, anti-postsynaptic density protein-95 (PSD-95) and Fluoro-Jade C were purchased from Chemicon Int., (Temecula, CA). Polyclonal anti-glial fibrillary acidic protein (GFAP), anti-synaptophysin, anti-β-actin, anti-calbindin, fluorescein isothiocyanate (FITC) conjugated-lectin and filipin were from Sigma (Oakville, ON, Canada), whereas α- and β-secretase assay kits were purchased from R & D Systems, Inc. (Minneapolis, MN). Polyclonal anti-cleaved caspase-3 was from Cell Signaling (Beverly, MA), neuron-specific marker NeuroTrace red fluorescent Nissl stain was from Invitrogen (Burlington, ON, Canada) and monoclonal anti-glyceraldehyde-3-phosphate dehydrogenase (GAPDH) antibody was from Abcam Inc. (Cambridge, MA). Secondary antisera such as donkey anti-rabbit Texas Red, donkey anti-rabbit FITC and donkey anti-mouse FITC were from Jackson ImmunoResearch (West Grove, PA) and IR800 donkey anti-rabbit and IR680 donkey anti-mouse antibodies were from LI-COR Inc. (Lincoln, NE). All other chemicals were from either Sigma or Fisher Scientific (Whitby, ON, Canada).

Npc1$^{-/-}$ and control mice

The *Npc1*$^{-/-}$ (n = 78) and age-matched control mice (n = 78) were obtained from a breeding colony of Balb/cNctr-*Npc*$^{N/+}$ mice set up at the University of Alberta after purchase of the original breeding pairs from Jackson Laboratories (Bar Harbor, ME, USA). The mice were maintained according to institutional guidelines and were supplied with food and water *ad libitum*. As *Npc1*$^{-/-}$ mice do not produce offspring, *Npc1* heterozygous (*Npc1*$^{+/-}$) mice were used to generate *Npc1*$^{-/-}$ and control (*Npc1*$^{+/+}$) mice. The *Npc1* genotype was determined from tail clippings by PCR analysis of genomic DNA (Karten et al., 2003). *Npc1*$^{-/-}$ and control mice from three different age groups (4-, 7- and 10-weeks old) were sacrificed by decapitation, their brains were rapidly removed and areas of interest (hippocampus and cerebellum) were dissected and frozen immediately in dry-ice for biochemical assays. For histological studies, *Npc1*$^{-/-}$ and control mice (4-, 7- and 10-weeks-old) were anesthetized with 8% chloral hydrate and then perfused with phosphate-buffered saline (PBS; 0.01M, pH 7.4), followed by 4% paraformaldehyde. Brains were sectioned (20 or 40 μm) on a cryostat and collected in a free-floating manner for further processing (Kodam et al., 2008).

Filipin Staining

Filipin specifically labels unesterified cholesterol (Boring and Geyer, 1974). Sections from *Npc1*$^{-/-}$ and control mouse brains were incubated in the dark with 125 μg/ml filipin in PBS for 3 h as described earlier (Amritraj et al., 2009a). In some cases, brain sections were first incubated overnight at 4°C with either FITC-conjugated lectin (1:100) or with anti-GFAP (1:100) antiserum, washed, exposed to Texas Red-conjugated secondary antibody (1:200) for 2 h and then incubated with filipin for 3 h. Stained sections were examined using a Zeiss Axioskop-2 microscope.

Fluoro-Jade C Staining

Fluoro-Jade C labels degenerating neurons, dendrites and axons (Schmued et al., 2005). Sections from 4-, 7- and 10-week-old *Npc1*$^{-/-}$ and control mouse brains were stained with 0.0001% Fluoro-Jade C in 0.1% acetic acid as described earlier (Amritraj et al., 2009a).

Immunoblotting

Brain tissues (hippocampus and cerebellum) from 4-, 7- and 10-week old *Npc1*$^{-/-}$ and control mice (4–6 animals/group) were homogenized in ice-cold radioimmunoprecipitation assay -lysis buffer [20 mM Tris–HCl (pH 8), 150 mM NaCl, 0.1% SDS, 1 mM EDTA, 1% Igepal CA-630, 50 mM NaF, 1 mM $NaVO_3$, 10 μg/ml leupeptin and 10 μg/ml aprotinin]. The proteins were separated by electrophoresis on 4–20% polyacrylamide gels and then transferred to nitrocellulose membranes. The membranes were blocked with 5% non-fat milk and incubated overnight at 4°C with anti-synaptophysin (1:1000), anti-PSD-95 (1:1000), anti-APP (369, 1:1000), anti-BACE1 (1:100), anti-PS1 (1:1000), anti-nicastrin (1:200), anti-PEN2 (1:500) or anti-APH1 (1:100) antibodies. Membranes were then incubated with the appropriate horseradish peroxidase (HRP)-conjugated secondary antibodies (1:5000) and developed using an enhanced chemiluminescence detection kit. Membranes were subsequently reprobed with anti-β-actin (1:1000) antibody and immunoreactive proteins were quantified using MCID image analysis system (Kodam et al., 2008). For the APP CTF analysis, 50 μg of total protein from hippocampal and cerebellar regions of *Npc1*$^{-/-}$ and control mice were separated on 16% Tris-Tricine gels and probed simultaneously with rabbit polyclonal CT15 (1:1000) and mouse anti-GAPDH (1:20,000) antibodies. The proteins were detected with IR800 anti-rabbit and IR680 anti-mouse secondary antibodies. Immunoblots were then quantified using Odessey Infrared Imaging system (LI-COR Inc., Licocoln, NE, USA). The data are presented as mean ± S.E.M. and were analyzed using the two-tailed t-test with significance set at $p < 0.05$.

Immunostaining

Brain sections from different age groups of *Npc1*$^{-/-}$ and control mice (3–5 animals/group) were processed as described earlier (Kodam et al., 2008). For the enzyme-linked procedure, 40 μm sections were treated with 1% hydrogen peroxide for 30 min and then incubated overnight at 4°C with anti-APP (CTM1, 1:500), anti-BACE1 (1:100), anti-PS1 (1:500), anti-nicastrin (1:500), anti-PEN2 (1:500) or anti-APH1 (1:100) antiserum. Sections were then exposed to HRP-conjugated secondary antibodies for 1 h, and developed using the glucose-oxidase-nickel enhancement method. Immunostained sections were examined using a Zeiss Axioskop-2 microscope.

For double immunofluorescence staining, brain sections (20 μm) from *Npc1*$^{-/-}$ and control mice of different age groups were incubated overnight with a combination of anti-APP (CTM1, 1:100), anti-nicastrin (1:100), anti-PS1 (1:200), anti-PEN2 (1:100), anti-BACE1 (1:50), anti-APH1 (1:50), anti-calbindin (1:3000) or NeuroTrace (1:300), in combination with FITC-conjugated lectin (1:100), anti-GFAP (1:500), anti-MAG (1:500) or anti-cleaved

caspase-3 (1:200) antisera. After incubation, sections were rinsed with PBS, exposed to Texas Red- or FITC-conjugated secondary antibodies (1:200), washed and mounted with Vectashield medium. Immunostained sections were examined under a Zeiss Axioskop-2 fluorescence microscope. To determine the number of reactive astrocytes expressing APP, morphometric analysis was carried out in both the hippocampus and cerebellum of 10-week-old *Npc1*$^{-/-}$ mice (n=4). For each animal, the number of GFAP-labeled astrocytes with or without APP was quantified using a 40X objective and a 10X eye-piece lenses on 5–8 fields from 6–8 consecutive sections (Amritraj et al., 2009b). Results obtained from all cases are presented as the percentage of reactive astrocytes expressing APP in the hippocampal and cerebellar regions.

Activity of α- and β-secretases

The hippocampus and cerebellum of 4-, 7- and 10-week-old *Npc1*$^{-/-}$ and control mice (4–6 animals/group) were processed to determine the activity of α-secretase and β-secretase using commercially available assay kits (Burns et al., 2003). Briefly, tissue samples were homogenized in sample buffer and added to a secretase-specific APP peptide substrates conjugated to the reporter molecules EDANS and DABCYL. In the uncleaved form, the fluorescent emissions from EDANS are quenched by the DABCYL moiety, whereas cleavage of the reporter peptide by the secretase separates the EDANS and DABCYL, allowing the release of a fluorescent signal. Thus, the level of secretase enzymatic activity in the homogenate is proportional to the fluorometric reaction measured at excitation/emission at 355/510 nm.

RESULTS

Altered cholesterol distribution, loss of neurons and glial activation in Npc1$^{-/-}$ mice

To determine the intracellular distribution of cholesterol in *Npc1*$^{-/-}$ mice, we performed filipin staining in brains of 4-, 7- and 10-week-old *Npc1*$^{-/-}$ and control mice (Fig. 1A–L). Little filipin staining was observed at any stage in either the hippocampus or cerebellum in control mice. However, filipin-labeled cholesterol was evident in most neurons of the hippocampus and cerebellum of 4-, 7- and 10-week-old *Npc1*$^{-/-}$ mice (Fig. 1A–D). Additionally, double labeling experiments revealed that most of the activated microglia and occasionally some reactive astrocytes were labeled with filipin in *Npc1*$^{-/-}$ mouse brains (Fig. 1E–L).

It was reported that *Npc1*$^{-/-}$ mice exhibit loss of neurons in defined regions of the brain such as the cerebellum, thalamus and brainstem but not in the hippocampus (German et al., 2001; Sarna et al., 2003). In keeping with these results we observed Fluoro-Jade C (Fig. 1M–P) and cleaved caspase-3-labelled (data not shown) cells in the cerebellum, but not in the hippocampus, of the *Npc1*$^{-/-}$ mouse brain. More of these degenerating cells were present at 4- and 7-weeks, but very few were observed in the 10-week-old cerebellum of *Npc1*$^{-/-}$ mice. We also observed a marked up-regulation of reactive astrocytes and microglia in the hippocampus and cerebellum of *Npc1*$^{-/-}$ mice compared to age-matched controls (Fig. 1E–H). The density of MAG-positive myelinated fibers, on the other hand, decreased progressively between 4- and 10-weeks in the *Npc1*$^{-/-}$ mouse brain (Fig. 1Q–T). Additionally, the presynaptic marker synaptophysin and post-synaptic marker PSD-95 were significantly decreased in an age-dependent manner in the cerebellum of *Npc1*$^{-/-}$ mouse brains. In the hippocampus, no marked alteration in synaptophysin level was evident at any stage, whereas the level of PSD-95 was decreased significantly only in 10-week-old *Npc1*$^{-/-}$ mice (Fig. 1U–X).

Levels and distribution of APP in Npc1$^{-/-}$ mice

To examine the possible involvement of Aβ-related peptides in NPC pathology, we evaluated the levels and expression of APP in the hippocampus and cerebellum of 4-, 7- and 10-week-old *Npc1*$^{-/-}$ mice compared to age-matched controls (Fig. 2). Our data revealed that APP levels in the hippocampus were significantly increased only in 10-week old *Npc1*$^{-/-}$ mice, whereas in the cerebellum a marked increase was evident in 7- as well as 10-week old *Npc1*$^{-/-}$ mice compared to age-matched controls (Fig. 2A–D). At the cellular level, APP immunoreactivity in control mice was distributed in neurons of the brain, as reported earlier (Beeson et al., 1994). The hippocampal formation exhibited intense immunoreactive APP primarily in CA1-CA3 pyramidal neurons and granule cells of the dentate gyrus. Occasionally, APP-immunoreactive neurons were apparent in the hilus region of the dentate gyrus (Fig. 2E). In the cerebellar region, most Purkinje cells showed APP expression in control brains (Fig. 2G). The overall expression of APP was modestly increased in the hippocampal neurons as well as in surviving cerebellar neurons in *Npc1*$^{-/-}$ mouse brains. Interestingly, a subset of GFAP-positive reactive astrocytes was found to express high levels of APP in the hippocampal and cerebellar regions of 4-, 7- and 10-week-old *Npc1*$^{-/-}$ mouse brains (Fig. 2I–P). Activated microglia did not express APP in brains of *Npc1*$^{-/-}$ mice at any age examined (Fig. 2Q–X). Quantitative analysis revealed that ~43% of hippocampal (GFAP, 71.3±2.7/field and GFAP+APP, 30.3±1.2/field) and ~54% of cerebellar (GFAP, 63.3±2.8/field and GFAP+APP, 34.3±3.5/field) astrocytes expressed APP in 10-week old *Npc1*$^{-/-}$ mouse brains.

Levels and distribution of BACE1 and γ-secretase components in Npc1$^{-/-}$ mice

To determine whether increased APP levels in *Npc1*$^{-/-}$ mouse brains were associated with a parallel increase in APP processing *via* the amyloidogenic pathway, we measured the levels/expression of BACE1 (Fig. 3) and subunits of the γ-secretase complex (Fig. 4–Fig. 7) in the hippocampus and cerebellum of *Npc1*$^{-/-}$ and control mice. Our results clearly showed that elimination of *Npc1* significantly increased BACE1 levels in the hippocampus only in 10-week-old *Npc1*$^{-/-}$ mice, whereas in the cerebellum the increase was apparent both in 7- and10-week-old *Npc1*$^{-/-}$ mice compared to age-matched controls (Fig. 3A–D). As for components of the γ-secretase complex, levels of PS1 (Fig. 4A–D) were significantly higher in the hippocampus and cerebellum of 10-week-old *Npc1*$^{-/-}$ mice. The steady-state levels of nicastrin (Fig. 5A–D), PEN2 (Fig. 6A–D) and APH1 (Fig. 7A–D), on the other hand, were enhanced by elimination of *Npc1* in mice from 7-weeks onwards in both the hippocampus and cerebellum.

At the cellular level, BACE1 (Fig. 3E, G) and γ-secretase components PS1 (Fig. 4E, G), nicastrin (Fig. 5E, G), PEN2 (Fig. 6E, G) and APH1 (Fig. 7E, G) were evident mostly in neurons in the normal brain. In the hippocampus, rather intense immunoreactivity was apparent in the CA1-CA3 pyramidal cell layer and in few medium-sized neurons scattered in the strata oriens and stratum radiatum. Within the dentate gyrus, granule cell somata were outlined by a fine mesh of weakly stained puncta and occasional strongly labeled neurons. In the cerebellum, immunoreactivity was evident in Purkinje cells as well as the granule cell layer. Double immunolabeling experiments of control mouse brains revealed that occasionally some astrocytes, but not microglia, exhibited BACE1 and PS1, but not nicastrin, PEN2 or APH1 immunoreactivity (data not shown). In comparison with the age-matched controls, the expression of BACE1, PS1, nicastrin, PEN2 and APH1 was modestly increased in the hippocampus as well as the cerebellum of *Npc1*$^{-/-}$ mouse brains from 7-week onwards. The increase was partly evident in hippocampal neurons as well as in the surviving cerebellar Purkinje cells. Interestingly, a subset of reactive astrocytes was found to express BACE1 (Fig. 3I–P), PS1 (Fig. 4I–P), nicastrin (Fig. 5I–P), PEN2 (Fig. 6I–P) and APH1 (Fig. 7I–P) in both the hippocampus and cerebellum of *Npc1*$^{-/-}$ mouse brains. The

relative number of reactive astrocytes expressing BACE1 and components of the γ-secretase complex was consistently higher in the cerebellum than the hippocampus. In contrast to astrocytes, activated microglia did not express either BACE1 (Fig. 3Q–X) or components of γ-secretase i.e., PS1 (Fig. 4Q–X), nicastrin (Fig. 5Q–X), PEN2 (Fig. 6Q–X) and APH1 (Fig. 7Q–X) in the hippocampus or cerebellum of brains of *Npc1*$^{-/-}$ mice of any age examined.

Activities of α- and β-secretases in Npc1$^{-/-}$ mice

To determine whether redistribution of cholesterol within brain cells can influence APP processing, we measured the activity of α- and β-secretases as well as the levels of α- and β-CTFs in the hippocampal and cerebellar regions of *Npc1*$^{-/-}$ and control mice (Fig. 8). While the activity of α-secretase was not altered by elimination of *Npc1* in 4-, 7- or 10-week-old mice (Fig. 8A, B), BACE activity was significantly higher in both the hippocampus and cerebellum of *Npc1*$^{-/-}$ mice at all age groups compared to the respective controls (Fig. 8C, D). Interestingly, the levels of α- and β-CTFs were not altered in the hippocampus at any age group of *Npc1*$^{-/-}$ mice, but were markedly elevated in the cerebellum of 10-week-old *Npc1*$^{-/-}$ mice (Fig. 8E–H).

DISCUSSION

The present study indicates that redistribution of cholesterol in NPC1 deficient mouse brains is associated with increased processing of APP, possibly leading to enhanced production of Aβ-related peptides. Our results reveal that i) *Npc1*$^{-/-}$ mice exhibit an age-dependent degeneration of neurons in the cerebellum but not in the hippocampus, *albeit* both regions show, activation of astrocytes as well as microglia, ii) cellular levels/expression of APP and BACE1, but not γ-secretase components, are increased by NPC1 deficiency earlier in the cerebellum than the hippocampus of the mouse brain, iii) a subset of reactive astrocytes in *Npc1*$^{-/-}$ mouse brains express higher levels of APP, BACE1 and γ-secretase and iv) β-secretase activity is markedly higher in the brain of *Npc1*$^{-/-}$ mice at all age groups, but levels of α- and β-CTFs are increased only in the cerebellum of 10-week-old *Npc1*$^{-/-}$ mice. Taken together, these results suggest that increased levels and processing of APP may be associated with the development of pathology and/or degenerative events that occur in *Npc1*$^{-/-}$ mouse brains.

Degeneration of neurons in Npc1$^{-/-}$ mice

Earlier studies have shown that *Npc1*$^{-/-}$ mice accumulate cholesterol within cells in almost all regions of the brain including the hippocampus and cerebellum as observed in the present study (Bi et al., 2005; Liao et al., 2007). However, severe loss of neurons is evident largely in the cerebellar Purkinje cells, whereas hippocampal neurons are relatively spared with the exception of some degenerating terminals in selected layers (German et al., 2001; Li et al., 2005; Sarna et al., 2003). At present, the underlying mechanisms associated with the loss of neurons remain unclear as events related to both apoptosis and autophagy have been identified in *Npc1*$^{-/-}$ mouse brains. Detection of TUNEL-positive and active caspase 3-immunoreactive Purkinje cells is consistent with cell death being due to apoptosis (Alvarez et al., 2008; Amritraj et al., 2009a; Wu et al., 2005). In keeping with these results, we also observed cleaved caspase-3 and Fluoro-Jade C-positive cells (i.e., Purkinje cells) in the cerebellum but not in the hippocampus of *Npc1*$^{-/-}$ mice. Interestingly, anti-apoptotic strategies, such as overexpression of Bcl-2 or treatment with minocycline, that are known to prevent apoptosis in some mouse models of neurodegenerative diseases, failed to protect neurons in *Npc1*$^{-/-}$ mice (Erickson and Bernard, 2002), raising the possibility that mechanisms other than apoptosis may be involved in NPC pathogenesis.

Influence of cholesterol accumulation on APP and its processing enzymes in Npc1$^{-/-}$ mice

Multiple lines of experiments have shown that elevated cholesterol levels can increase Aβ production, whereas inhibition of cholesterol synthesis can lower Aβ levels (Fassbender et al., 2001; Frears et al., 1999; Puglielli et al., 2003; Simons et al., 1998; Yamazaki et al., 2001). It is suggested that the critical factor influencing Aβ production may not be total cholesterol levels, but rather the ratio of free cholesterol to cholesterol ester, or the compartmentalization of cholesterol within the cell (see Puglielli et al., 2003). Considering the evidence that a subset of cellular APP, as well as β- and γ-secretases, are localized in cholesterol-rich lipid-raft domains (Tun et al., 2002; Vetrivel et al., 2004; Wahrle et al., 2002), it is likely that an increased level or an altered distribution of cholesterol enhances amyloidogenic APP processing leading to increased Aβ production. Consistent with these results, we observed a significant increase in the level/expression of APP and its processing enzymes, as well as activity of the enzyme BACE, in both the hippocampus and cerebellum of *Npc1*$^{-/-}$ mice, thus suggesting an overall increase in amyloidogenic potential. Interestingly, increased APP and BACE1 levels were evident earlier in the more vulnerable cerebellar region than in the hippocampus of *Npc1*$^{-/-}$ mice. Additionally, the levels of α- and β-CTFs were found to be significantly increased only in the cerebellum of 10-week-old *Npc1*$^{-/-}$ mice. While the increased levels of β-CTF may represent enhanced production/accumulation within cerebellar neurons (Jin et al., 2004), the significance of the increase in α-CTF in *Npc1*$^{-/-}$ mice remains unclear. Given the evidence that α-secretase activity is not altered and lysosomal functions are severely impaired in the cerebellum of *Npc1*$^{-/-}$ mice (Amritraj et al., 2009a; Liao et al., 2007), it is possible that increased α-CTF levels may reflect decreased lysosomal clearance of this polypeptide. Studies from cultured neurons revealed that cholesterol accumulation, following treatment with a class II amphiphilic drug U18666A, can lead to increased Aβ production and loss of neurons (Koh and Cheung, 2006; Yamazaki et al., 2001; but see Davis, 2008; Runz et al., 2002). There is also evidence that *Npc1*$^{-/-}$ mice can exhibit increased production of Aβ peptides that may be associated with the redistribution of PS1 to early endosomes and increased γ-secretase activity (Burns et al., 2003; Yamazaki et al., 2001). However, an earlier study which used hemibrain tissues, without cerebellum and brainstem from *Npc1*$^{-/-}$ mice (Burns et al., 2003), did not report any alteration in the levels of APP or BACE1 as observed in the present study. It is possible that APP and BACE1 levels are altered regionally, but these changes were masked in the whole brain lysate assay employed in the previous study

In control brains APP, BACE1 and γ-secretase components are usually localized in neurons of the hippocampus and cerebellum but not in glial cells (Beeson et al., 1994; Kodam et al., 2008; Rossner et al., 2001; Siman and Salidas, 2004; Sun et al., 2002). The present study showed that expression of APP and its processing enzymes is moderately increased in neurons of *Npc1*$^{-/-}$ mice compared to control mice in an age-dependent manner. Additionally, a subset of reactive astrocytes was consistently found to express higher levels of APP and its processing enzymes in the hippocampus and cerebellum of *Npc1*$^{-/-}$ mouse brains. The number of these astrocytes increased with the progression of disease pathology and was more evident in the cerebellum than in the hippocampus of *Npc1*$^{-/-}$ mice. At present, however, it remains unclear to what extent reactive astrocytes can accumulate Aβ-related peptides or contribute to the increased production/levels of Aβ peptides in *Npc1*$^{-/-}$ mouse brains. Some earlier studies have reported that expression of APP, BACE, PS1 and/or nicastrin can be induced in activated astrocytes following a variety of brain lesion paradigms such as cerebral ischemia, traumatic brain injury and kainic acid-induced excitotoxicity (Banati et al., 1995; Hartlage-Rubsamen et al. 2003; Nadler et al., 2008). There is also evidence that activated astrocytes located in close proximity to Aβ-containing neuritic plaques in AD brains and transgenic mice overproducing Aβ peptide express higher levels of

APP and/or its processing enzymes (Hartlage-Rubsamen et al., 2003). Thus, the increased expression of APP and its processing enzymes in a subset of reactive astrocytes observed in the present study might not be specific to NPC pathology but could be a general phenomenon that results from or accompanies neurodegenerative events and/or chronic gliosis. It is possible that factors released from activated microglia and/or damaged neurons trigger astrocytic expression of APP and its processing enzymes (Rossner et al., 2005).

Possible implication of Aβ-related peptides in Npc1$^{-/-}$ mice

Earlier studies have shown that the cerebellum is most severely affected in NPC disease with profound loss of neurons, whereas the hippocampus displays some degenerating terminals without significant neuronal loss (Amritraj et al., 2009a; Li et al., 2005; Sarna et al., 2003). The present study revealed that levels of APP and BACE1 were increased earlier in the cerebellum than hippocampus and that components of γ-secretase are enhanced concomitantly in both the regions in response to NPC1 deficiency. This increase can be attributed partly to reactive astrocytes which are known to play a critical role in regulating disease pathogenesis. These results, together with increased BACE activity, suggest that enhanced production as well as accumulation of β-CTF and/or Aβ-related peptides may appear earlier in the cerebellum in *Npc1*$^{-/-}$ mice (Burns et al., 2003; Jin et al., 2004). Although intraneuronal accumulation of Aβ-related peptides has been hypothesized to be toxic to neurons in AD pathology (Wirths et al., 2004; Zhang et al., 2002), the implication of increased β-CTF or Aβ peptides in NPC pathology remains unclear. It has been shown that in NPC disease, the surviving Purkinje cells contain a significant amount of β-CTF/Aβ-related peptide, whereas the hippocampus displays only some accumulation of $A\beta_{1-42}$ (Jin et al., 2004). Thus, it is possible that lack of overt neurodegeneration in the hippocampus of *Npc1*$^{-/-}$ mice may be associated with a higher threshold level, a later appearance and/or faster clearance of β-CTF/Aβ-related peptides, whereas increased level/accumulation or earlier generation of these peptides might cause the observed loss of neurons in the cerebellum. There is also evidence that Aβ peptides generated by astrocytes might contribute to the loss of neurons. This is supported by data showing that pharmacological treatments attenuating loss of neurons and/or disease pathology in animal models of neurodegeneration are accompanied by decreased level/expression of APP or its processing enzymes in reactive astrocytes (Lee et al., 2008; Panegyres and Hughes, 1998; Yamamoto et al., 2007). In summary, we have demonstrated that altered distribution of cholesterol can increase the levels/expression of APP and its processing enzymes, in both neurons and in reactive astrocytes, which might contribute either directly or indirectly to the pathological features associated with NPC disease.

Abbreviations

Aβ	amyloid β
AD	Alzheimer’s disease
APH1	anterior pharynx defective 1
APP	amyloid precursor protein
BACE	β-site APP cleaving enzyme
CTF	C-terminal fragment
EL	endosomal-lysosomal
FITC	fluorescein isothiocyanate
GAPDH	glyceraldehyde-3-phosphate dehydrogenase

GFAP	glial fibrillary acidic protein
HRP	horseradish peroxidase
MAG	myelin associated glycoprotein
NPC	Niemann-Pick type C
PBS	phosphate-buffered saline
PEN2	presenilin enhancer 2
PSD-95	postsynaptic density-95
PS1/2	presenilins 1/2

Acknowledgments

This work is supported by grants from the Canadian Institutes of Health Research (SK and JEV), Ara Parseghian Medical Research Foundation (JEV), Alzheimer's Association grant NIRG (KSV) and National Institutes of Health Grants AG021495 and AG019070 (GT). MM is a recipient of President's International Doctoral award from the University of Alberta and a studentship award from the Alberta Heritage Foundation for Medical Research (AHFMR). KP is a recipient of studentship award from the AHFMR and Natural Sciences and Engineering Research Council of Canada. SK is a recipient of Canada Research Chair (Tier-II).

REFERENCES

Amritraj A, Peake K, Kodam A, Salio C, Merighi A, Vance JE, Kar S. Increased activity and altered subcellular distribution of lysosomal enzymes determine neuronal vulnerability in Niemann-Pick type C1-deficient mice. Am J Pathol. 2009a; 175:2540–2556. [PubMed: 19893049]

Amritraj A, Hawkes C, Phinney AL, Mount HT, Scott CD, Westaway D, Kar S. Altered levels and distribution of IGF-II/M6P receptor and lysosomal enzymes in mutant APP and APP+PS1 transgenic mouse brains. Neurobiol Aging. 2009b; 30:54–70. [PubMed: 17561313]

Alvarez AR, Klein A, Castro J, Cancino GI, Amigo J, Mosqueira M, Vargas LM, Yévenes LF, Bronfman FC, Zanlungo S. Imatinib therapy blocks cerebellar apoptosis an improves neurological symptoms in a mouse model of Niemann-Pick type C disease. FASEB J. 2008; 10:3617–3627. [PubMed: 18591368]

Banati RB, Gehrmann J, Wiessner C, Hossmann KA, Kreutzberg GW. Glial expression of the β-amyloid precursor protein (APP) in global ischemia. J Cereb Blood Flow Metab. 1995; 15:647–654. [PubMed: 7790414]

Baudry M, Yao Y, Simmons D, Liu J, Bi X. Postnatal development of inflammation in a murine model of Niemann-Pick type C disease: immunohistochemical observations of microglia and astroglia. Exp Neurol. 2003; 184:887–903. [PubMed: 14769381]

Beeson JG, Shelton ER, Chan HW, Gage FH. Differential distribution of amyloid protein precursor immunoreactivity in the rat brain studied by using five different antibodies. J Comp Neurol. 1994; 342:78–96. [PubMed: 8207129]

Bi X, Liu J, Yao Y, Baudry M, Lynch G. Deregulation of the phosphatidylinositol-3 kinase signaling cascade is associated with neurodegeneration in Npc1$^{-/-}$mouse brain. Am J Pathol. 2005; 67:1081–1092. [PubMed: 16192643]

Bornig H, Geyer G. Staining of cholesterol with the fluorescent antibiotic "filipin". Acta Histochem. 1974; 50:110–115. [PubMed: 4140671]

Burns M, Gaynor K, Olm V, Mercken M, LaFrancois J, Wang L, Mathews PM, Noble W, Matsuoka Y, Duff K. Presenilin redistribution associated with aberrant cholesterol transport enhances β-amyloid production in vivo. J Neurosci. 2003; 23:5645–5649. [PubMed: 12843267]

Carstea ED, Morris JA, Coleman KG, Loftus SK, Zhang D, Cummings C, Gu J, Rosenfeld MA, Pavan WJ, Krizman DB, Nagle J, Polymeropoulos MH, Sturley SL, Ioannou YA, Higgins ME, Comly M, Cooney A, Brown A, Kaneski CR, Blanchette-Mackie EJ, Dwyer NK, Neufeld EB, Chang TY, Liscum L, Strauss JF 3rd, Ohno K, Zeigler M, Carmi R, Sokol J, Markie D, O'Neill RR, van

Diggelen OP, Elleder M, Patterson M, Brady RO, Vanier MT, Pentchev PG, Tagle DA. Niemann-Pick C1 disease gene: homology to mediators of cholesterol homeostasis. Science. 1997; 277:228–231. [PubMed: 9211849]

Clippingdale AB, Wade JD, Barrow CJ. The amyloid-β peptide and its role in Alzheimer's disease. J Peptide Sci. 2001; 7:227–249. [PubMed: 11428545]

Cole SL, Vassar R. The role of amyloid precursor protein processing by BACE1, the β-secretase in Alzheimer's disease pathology. J Biol Chem. 2008; 283:29621–29625. [PubMed: 18650431]

Davis W. The cholesterol transport inhibitor U18666a regulates amyloid precursor protein metabolism and trafficking in N2aAPP "Swedish" cells. Curr Alz Res. 2008; 5:448–456.

Erickson RP, Bernard O. Studies on neuronal death in the mouse model of Niemann-Pick C disease. J Neurosci Res. 2002; 68:738–744. [PubMed: 12111834]

Fassbender K, Simons M, Bergmann C. Simvastatin strongly reduces Alzheimer`s disease Aβ42 and Aβ40 levels *in vitro* and *in vivo*. Proc Natl Acad Sci USA. 2001; 98:5856–5861. [PubMed: 11296263]

Frears ER, Stephens DJ, Walters CE, Davies H, Austen BM. The role of cholesterol in the biosynthesis of β-amyloid. Neuroreport. 1999; 10:1699–1705. [PubMed: 10501560]

German DC, Quintero EM, Liang CL, Ng B, Punia S, Xie C, Dietschy JM. Selective neurodegeneration, without neurofibrillary tangles, in a mouse model of Niemann-Pick C disease. J Comp Neurol. 2001; 433:415–425. [PubMed: 11298365]

Hartlage-Rubsamen M, Zeitschel U, Apelt J, Gartner U, Franke H, Stahl T, Gunther A, Schliebs R, Penkowa M, Bigl V, Rossner S. Astrocytic expression of the Alzheimer's disease β-secretase (BACE1) is stimulus-dependent. Glia. 2003; 41:169–179. [PubMed: 12509807]

Jin L, Maezawa I, Vincent I, Bird T. Intracellular accumulation of amyloidogenic fragments of amyloid-β precursor protein in neurons with Niemann-Pick type C defects is associated with endosomal abnormalities. Am J Pathol. 2004; 164:975–985. [PubMed: 14982851]

Kar S, Slowikowski SP, Westaway D, Mount HTJ. Beta-amyloid peptide and central cholinergic neurons: functional interrelationships and possible implications in Alzheimer's disease pathology. J Psychiat Neurosci. 2004; 29:427–441.

Karten B, Vance DE, Campenot RB, Vance JE. Trafficking of cholesterol from cell bodies to distal axons in Niemann Pick C1 deficient neurons. J Biol Chem. 2003; 278:4168–4175. [PubMed: 12458210]

Kodam A, Vetrivel KS, Thinakaran G, Kar S. Cellular distribution of g-secretase subunit nicastrin in the developing and adult rat brains. Neurobiol Aging. 2008; 29:724–738. [PubMed: 17222950]

Koh CH, Cheung NS. Cellular mechanism of U18666A–mediated apoptosis in cultured murine cortical neurons: bridging Niemann-Pick disease type C and Alzheimer's disease. Cell Signal. 2006; 18:1844–1853. [PubMed: 16797161]

Lee JW, Lee YK, Yuk DY, Choi DY, Ban SB, Oh KW, Hong JT. Neuro-inflammation induced by lipopolysaccharide causes cognitive impairment through enhancement of β-amyloid generation. J Neuroinflammation. 2008; 5:1–14. [PubMed: 18171484]

Li H, Repa JJ, Valasek MA, Beltroy EP, Turley SD, German DC, Dietschy JM. Molecular, anatomical, and biochemical events associated with neurodegeneration in mice with Niemann-Pick type C disease. J Neuropathol Exp Neurol. 2005; 64:323–333. [PubMed: 15835268]

Liao G, Yao Y, Liu J, Yu Z, Cheung S, Xie A, Liang X, Bi X. Cholesterol accumulation is associated with lysosomal dysfunction and autophagic stress in $Npc1^{-/-}$ mouse brain. Am J Pathol. 2007; 171:962–975. [PubMed: 17631520]

Loftus SK, Morris JA, Carstea ED, Gu JZ, Cummings C, Brown A, Ellison J, Ohno K, Rosenfeld MA, Tagle DA, Pentchev PG, Pavan WJ. Murine model of Niemann-Pick C disease: mutation in a cholesterol homeostasis gene. Science. 1997; 277:232–235. [PubMed: 9211850]

Mukerjee S, Maxfield FR. Lipid and cholesterol trafficking in NPC. Biochimica et Biophysica Acta. 2004; 1685:28–37. [PubMed: 15465424]

Nadler Y, Alexandrovich A, Grigoriadis N, Hartmann T, Rao KS, Shohami, Stein R. Increased expression of the γ-secretase components presenilin-1 and nicastrin in activated astrocytes and microglia following traumatic brain injury. Glia. 2008; 56:552–567. [PubMed: 18240300]

Nixon RA. Niemann-Pick type C disease and Alzheimer's disease: the APP-endosome connection fattens up. Am J Pathol. 2004; 164:757–761. [PubMed: 14982829]

Pacheco CD, Lieberman AP. The pathogenesis of Niemann-Pick type C disease: a role for autophagy? Expert Rev Mol Med. 2008; 10:1–14.

Panegyres PK, Hughes J. The neuroprotective effects of the recombinant interleukin-1 receptor antagonist rhIL-1ra after excitotoxic stimulation with kainic acid and its relationship to the amyloid precursor protein gene. J Neurol Sci. 1998; 154:123–132. [PubMed: 9562301]

Paul CA, Boegle AK, Maue RA. Before the loss: neuronal dysfunction in Niemann-Pick Type C disease. Biochimica et Biophysica Acta. 2004; 1685:63–76. [PubMed: 15465427]

Pentchev, PV.; Vanier, MT.; Suzuki, K.; Patterson, MC. Niemann-Pick disease type C: a cellular cholesterol lipidosis. In: Scriver, CR.; Beaudet, AL.; Sly, WS.; Valle, D., editors. The Metabolic and Molecular Basis of Inherited Disease. Vol. Vol. II. McGraw-Hill, New York: 1995. p. 2625-2639.

Puglielli L, Tanzi RE, Kovacs DM. Alzheimer's disease: the cholesterol connection. Nat Neurosci. 2003; 6:345–351. [PubMed: 12658281]

Reid PC, Urano Y, Kodama T, Hamakubo T. Alzheimer's disease: cholesterol, membrane rafts, isoprenoids and statins. J Cell Mol Med. 2007; 11:383–392. [PubMed: 17635634]

Rossner S, Apelt J, Schliebs R, Perez-Polo JR, Bigl V. Neuronal and glial β-secretase (BACE) protein expression in transgenic Tg2576 mice with amyloid plaque pathology. J Neurosci Res. 2001; 64:437–446. [PubMed: 11391698]

Rossner S, Lange-Dohna C, Zeitschel U, Perez-Polo JR. Alzheimer's disease β-secretase BACE1 is not a neuron-specific enzyme. J Neurochem. 2005; 92:226–234. [PubMed: 15663471]

Runz H, Rietdorf J, Tomic I, de Bernard M, Beyreuther K, Pepperkok R, Hartmann T. Inhibition of intracellular cholesterol transport alters presenilin localization and amyloid precursor protein processing in neuronal cells. J Neurosci. 2002; 22:1679–1689. [PubMed: 11880497]

Sarna JR, Larouche M, Marzban H, Sillitoe RV, Rancourt DE, Hawkes R. Patterned Purkinje cell degeneration in mouse models of Neimann-Pick type C disease. J Comp Neurol. 2003; 456:279–291. [PubMed: 12528192]

Schmued LC, Stowers CC, Scallet AC, Xu L. Fluoro-Jade C results in ultra high resolution and contrast labeling of degenerating neurons. Brain Res. 2005; 1035:24–31. [PubMed: 15713273]

Selkoe DJ. Biochemistry and molecular biology of amyloid β-protein and mechanism of Alzheimer's disease. Handb Clin Neurol. 2008; 89:245–260. [PubMed: 18631749]

Simons M, Keller P, De Strooper B, Beyreuther K, Dotti C, Simons K. Cholesterol depletion inhibits the generation of β-amyloid in hippocampal neurons. Proc Natl Acad Sci USA. 1998; 95:6460–6464. [PubMed: 9600988]

Siman R, Salidas S. Gamma-secretase subunit composition and distribution in the presenilin wild-type and mutant mouse brain. Neuroscience. 2004; 129:615–628. [PubMed: 15541883]

Steiner H, Fluhrer R, Haass C. Intramembrane proteolysis by gamma-secretase. J Biol Chem. 2008; 283:29627–29631. [PubMed: 18650432]

St George-Hyslop PH, Petit A. Molecular biology and genetics of Alzheimer's disease. CR Biologies. 2005; 328:119–130.

Sun A, Koelsch G, Tang J, Bing G. Localization of beta-secretase memapsin 2 in the brain of Alzheimer's patients and normal aged controls. Exp Neurol. 2002; 175:10–22. [PubMed: 12009756]

Thinakaran G, Koo EH. Amyloid precursor protein trafficking, processing and function. J Biol Chem. 2008; 283:29615–29619. [PubMed: 18650430]

Tun H, Marlow L, Pinnix I, Kinsey R, Samamurti K. Lipid rafts play an important role in Aβ biogenesis by regulating the β-secretase pathway. J Mol Neurosci. 2002; 19:31–35. [PubMed: 12212790]

Vance JE. Lipid imbalance in the neurological disorder, Niemann-Pick C disease. FEBS Lett. 2006; 580:5518–5524. [PubMed: 16797010]

Vanier MT, Suzuki K. Recent advances in elucidating Niemann-Pick C disease. Brain Pathol. 1998; 8:163–174. [PubMed: 9458174]

Vetrivel KS, Cheng H, Lin W, Sakurai T, Li T, Nukina N, Wong PC, Xu H, Thinakaran G. Association of γ-secretase with lipid rafts in post-Golgi and endosome membranes. J Biol Chem. 2004; 279:44945–44954. [PubMed: 15322084]

Vetrivel KS, Meckler X, Chen Y, Nguyen PD, Seidah NG, Vassar R, Wong PC, Fukata M, Kounnas MZ, Thinakaran G. Alzheimer disease Aβ production in the absence of S-palmitoylation-dependent targeting of BACE1 to lipid rafts. J Biol Chem. 2009; 284:3793–3803. [PubMed: 19074428]

Wahrle S, Das P, Nyborg AC, McLendon C, Shoji M, Kawarabayashi T, Younkin LH, Younkin SG, Golde TE. Cholesterol-dependent γ-secretase activity in buoyant cholesterol-rich membrane microdomains. Neurobiol Dis. 2002; 9:11–23. [PubMed: 11848681]

Walkley SU, Suzuki K. Consequences of NPC1 and NPC2 loss of function in mammalian neurons. Biochimica et Biophysica Acta. 2004; 1685:48–62. [PubMed: 15465426]

Wirths O, Multhaup G, Bayer TA. A modified beta-amyloid hypothesis: intraneuronal accumulation of the beta-amyloid peptide--the first step of a fatal cascade. J Neurochem. 2004; 91:513–520. [PubMed: 15485483]

Wu YP, Mizukami H, Matsuda J, Saito Y, Proia R, Suzuki K. Apoptosis accompanied by up-regulation of TNF-a death pathway genes in the brain of Niemann-Pick type C disease. Mol Genet Metab. 2005; 84:9–17. [PubMed: 15639190]

Yamamoto M, Kiyota T, Horiba M, Buescher JL, Walsch SM, Gendelman HE, Ikezu T. Interferon-γ and tumor necrosis factor-α regulate amyloid β plaque deposition and β-secretase expression in Swedish mutant APP transgenic mice. Am J Pathol. 2007; 170:680–692. [PubMed: 17255335]

Yamazaki T, Chang T-Y, Haass C, Ihara Y. Accumulation and aggregation of amyloid β-protein in late endosomes of Niemann-Pick type C cells. J Biol Chem. 2001; 276:4454–4460. [PubMed: 11085995]

Zhang Y, McLaughlin R, Goodyer C, LeBlanc A. Selective cytotoxicity of intracellular amyloid beta peptide1–42 through p53 and Bax in cultured primary human neurons. J Cell Biol. 2002; 156:519–529. [PubMed: 11815632]

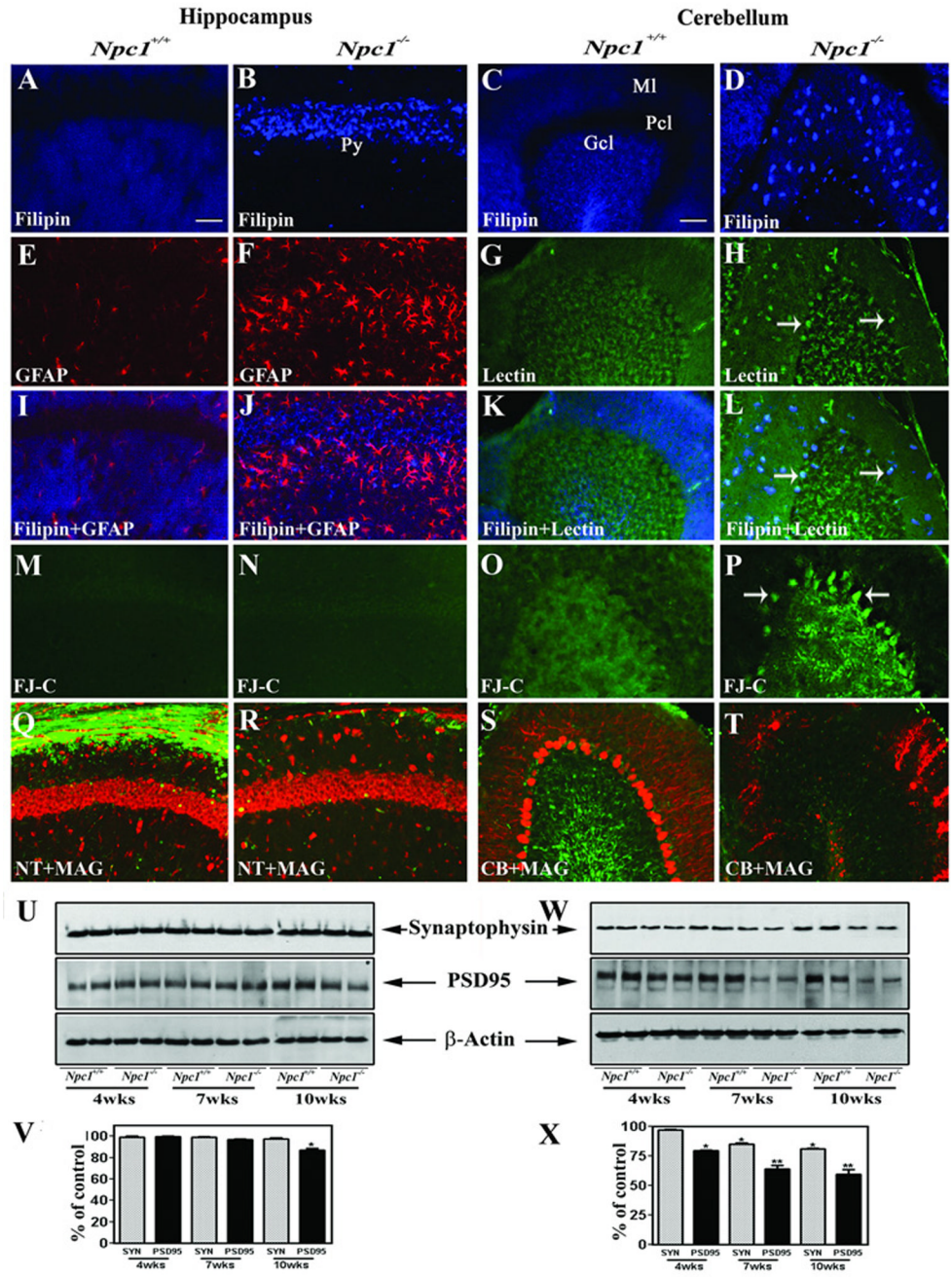

Fig. 1.

A–D; Photomicrographs demonstrating the accumulation of cholesterol in the hippocampus (A, B) and cerebellum (C, D) of the 10-week-old *Npc1*$^{-/-}$ (B, D) but not in control (*Npc1*$^{+/+}$; A, C) mice. E–L; Photomicrographs showing filipin labeling in astrocytes (red) in the hippocampus (E, F, I, J) and microglia (green) in the cerebellum (G, H, K, L) of 10-week-old control (*Npc1*$^{+/+}$; E, I, G, K) and *Npc1*$^{-/-}$ (F, J, H, L) mice. Note that almost all microglia exhibit filipin labeling (arrows), whereas only few astrocytes displayed filipin staining. M–P; Photomicrographs depicting degenerating neurons in the cerebellum (O, P) but not in the hippocampus (M, N) of *Npc1*$^{-/-}$ mice as revealed by Fluoro-Jade C staining. Q–T; Double immunofluorescence photomicrographs showing neurotrace (NT)/calbindin

(CB) labeled neurons (red) and MAG-labeled myelinated fibers (green) in the hippocampus (Q, R) and cerebellum (S, T) of 10-week-old control ($Npc1^{+/+}$; Q, S) and $Npc1^{-/-}$ (R, T) mouse brains. U–X; Immunoblots and respective histograms showing the altered levels of synaptophysin (SYN) and PSD-95 in the hippocampus (U, V) and cerebellum (W, X) of 4-, 7- and 10-week (wk) old $Npc1^{-/-}$ mouse brains compared to age-matched controls ($Npc1^{+/+}$). Histograms represent quantification of data from three separate experiments, each of which was replicated 2–3 times. Py, pyramidal cell layer; Ml, molecular layer; Gcl, granular cell layer; Pcl, Purkinje cells. Scale bar = 50 μM. *$p<0.05$, **$p<0.01$.

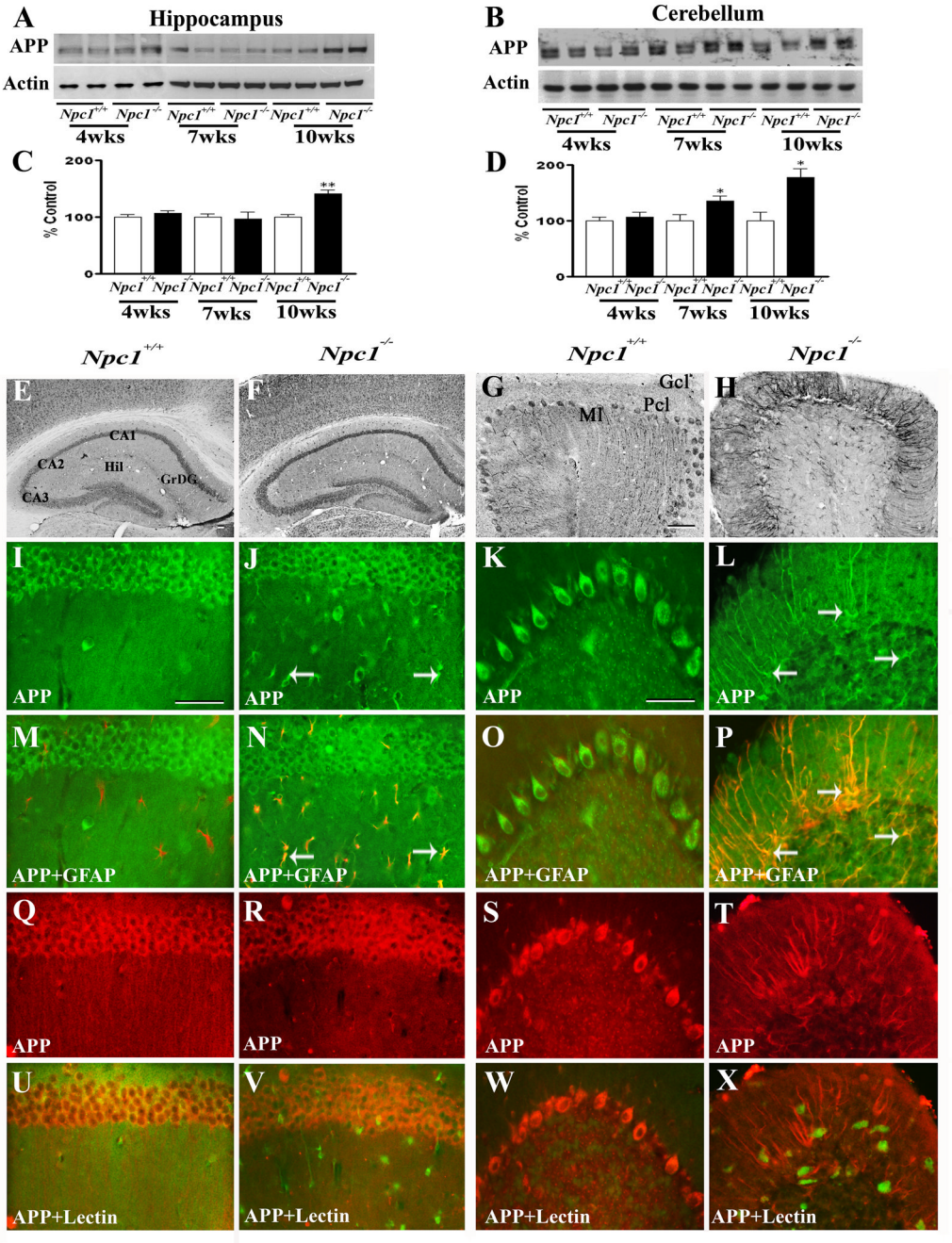

Fig. 2.

A–D; Immunoblots (A, B) and histograms (C, D) showing the level of APP in the hippocampus (A, C) and cerebellum (B, D) of 4-, 7- and 10-week- (wk) old *Npc1*$^{-/-}$ mice compared to controls (*Npc1*$^{+/+}$). E–H; Photomicrographs depicting the loss of APP-positive neurons in the cerebellum (G, H) but not in the hippocampus (E, F) of 10-wk-old *Npc1*$^{-/-}$ (F, H) mice compared to control (*Npc1*$^{+/+}$; E, G) mice. I–X; Double labeling showing that APP (I–L, Q–T) is not expressed in astrocytes (M, O) or microglia (U, W) in 10-wk-old hippocampus (M, U) or cerebellum (O, W) of *Npc1*$^{+/+}$ mice, whereas a number of reactive astrocytes (arrows; N, P) but not microglia (V, X) exhibit APP immunoreactivity in *Npc1*$^{-/-}$ hippocampus (N, V) and cerebellum (P, X). Histograms represent quantification of APP

levels from at least 3 separate experiments. Hil, hilus; GrDG, granule cells of the dentate gyrus; Ml, molecular layer; Gcl, granular cell layer; Pcl, Purkinje cells. Scale bar = 50 μM. *p<0.05, **p<0.01.

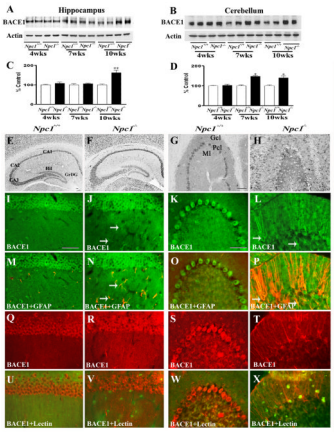

Fig. 3.

A–D; Immunoblots (A, B) and histograms (C, D) showing the level of BACE1 in the hippocampus (A, C) and cerebellum (B, D) of 4-, 7- and 10-week- (wk) old *Npc1*$^{-/-}$ mice compared to controls (*Npc1*$^{+/+}$). E–H; Photomicrographs depicting the loss of BACE1-positive neurons in the cerebellum (G, H) but not in the hippocampus (E, F) of 10-wk-old *Npc1*$^{-/-}$ (F, H) mice compared to controls (*Npc1*$^{+/+}$; E, G). I–X; Double labeling showing that BACE1 (I–L, Q–T) is not expressed in astrocytes (M, O) or microglia (U, W) in 10-wk-old hippocampus (M, U) or cerebellum (O, W) of *Npc1*$^{+/+}$ mice, whereas some astrocytes (arrows; N, P) but not microglia (V, X) exhibit BACE1 immunoreactivity in *Npc1*$^{-/-}$ hippocampus (N, V) and cerebellum (P, X). Histograms represent BACE1 levels from 3 experiments. Abbreviations are same as Fig. 2. Scale bar = 50 μM. *p<0.05, **p<0.01.

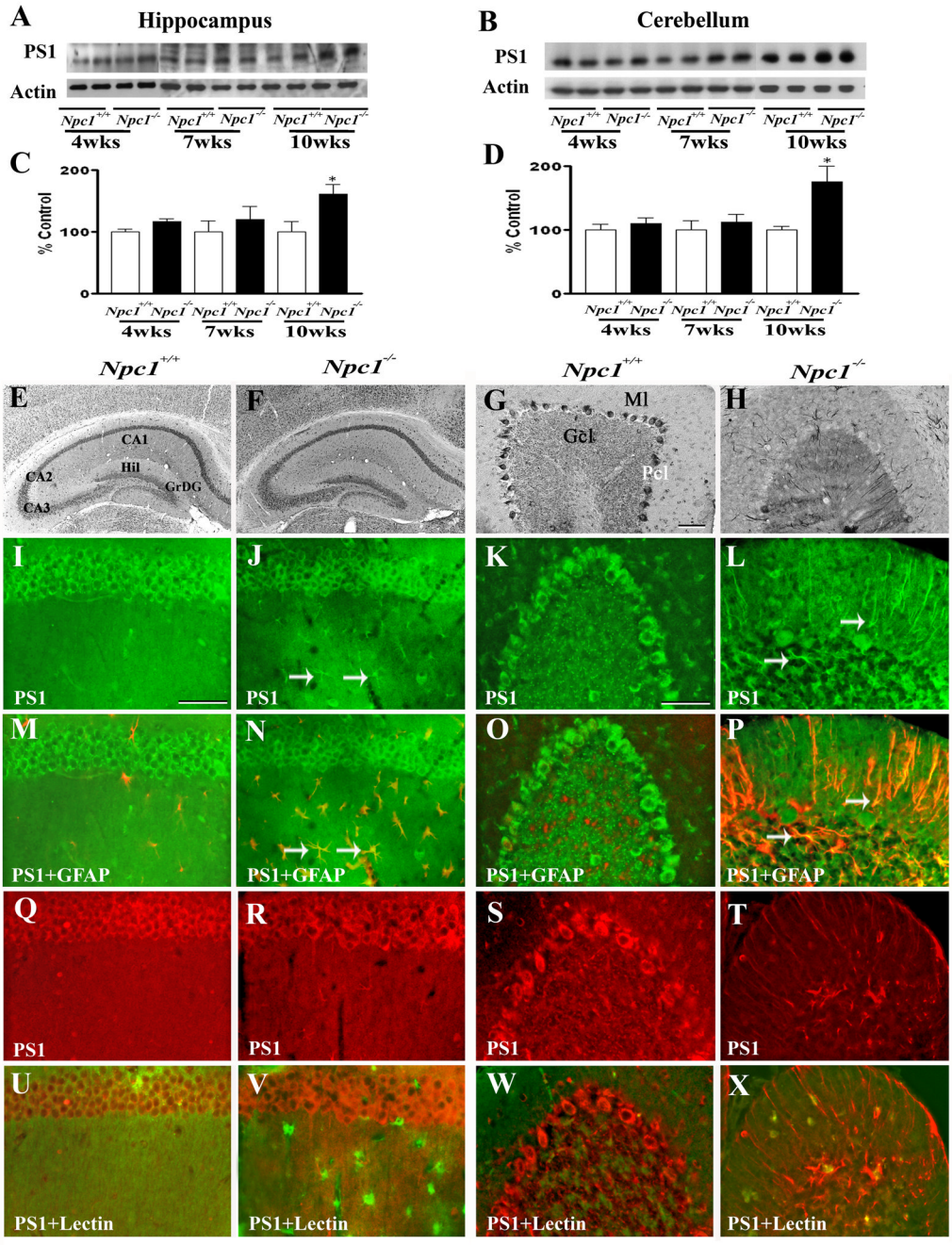

Fig. 4.

A–D; Immunoblots (A, B) and histograms (C, D) showing the level of PS1 in the hippocampus (A, C) and cerebellum (B, D) of 4-, 7- and 10-week- (wk) old *Npc1*$^{-/-}$ mice compared to controls (*Npc1*$^{+/+}$). E–H; Photomicrographs depicting the loss of PS1-positive neurons in the cerebellum (G, H) but not in the hippocampus (E, F) of 10-wk-old *Npc1*$^{-/-}$ (F, H) mice compared to controls (*Npc1*$^{+/+}$; E, G). I–X; Double labeling showing that PS1 (I–L, Q–T) is not expressed in astrocytes (M, O) or microglia (U, W) in 10-wk-old hippocampus (M, U) or cerebellum (O, W) of *Npc1*$^{+/+}$ mice, whereas some reactive astrocytes (arrows; N, P) but not microglia (V, X) exhibit PS1 immunoreactivity in *Npc1*$^{-/-}$ hippocampus (N, V) and cerebellum (P, X). Histograms represent PS1 levels from 3

separate experiments. Abbreviations are same as Fig. 2. Scale bar = 50 μM. *p<0.05, **p<0.01.

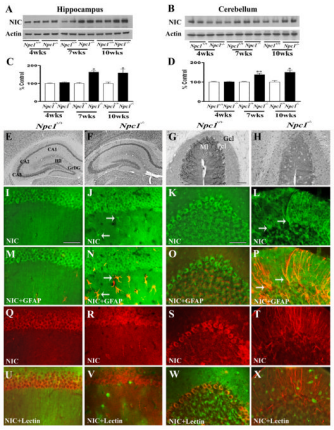

Fig. 5.

A–D; Immunoblots (A, B) and histograms (C, D) showing the level of nicastrin (NIC) in the hippocampus (A, C) and cerebellum (B, D) of 4-, 7- and 10-week- (wk) old *Npc1*$^{-/-}$ mice compared to controls (*Npc1*$^{+/+}$). E–H; Photomicrographs depicting the loss of NIC-positive neurons in the cerebellum (G, H) but not in the hippocampus (E, F) of 10-wk-old *Npc1*$^{-/-}$ (F, H) mice compared to controls (*Npc1*$^{+/+}$; E, G). I–X; Double labeling showing that NIC (I–L, Q–T) is not expressed in astrocytes (M, O) or microglia (U, W) in 10-wk-old hippocampus (M, U) or cerebellum (O, W) of *Npc1*$^{+/+}$ mice, whereas some astrocytes (arrows; N, P) but not microglia (V, X) exhibit NIC immunoreactivity in *Npc1*$^{-/-}$ hippocampus (N, V) and cerebellum (P, X). Histograms represent NIC levels from 3 experiments. Abbreviations are same as Fig. 2. Scale bar = 50 μM. *p<0.05, **p<0.01.

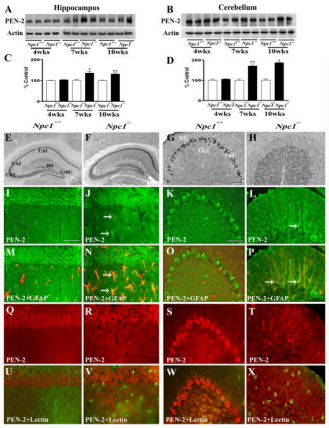

Fig. 6.

A–D; Immunoblots (A, B) and histograms (C, D) showing the level of presenilin enhancer 2 (PEN2) in the hippocampus (A, C) and cerebellum (B, D) of 4-, 7- and 10-week- (wk) old *Npc1*$^{-/-}$ mice compared to controls (*Npc1*$^{+/+}$). E–H; Photomicrographs depicting the loss of PEN2-positive neurons in the cerebellum (G, H) but not in the hippocampus (E, F) of 10-wk-old *Npc1*$^{-/-}$ (F, H) mice compared to controls (*Npc1*$^{+/+}$; E, G). I–X; Double labeling showing that PEN2 (I–L, Q–T) is not expressed in astrocytes (M, O) or microglia (U, W) in 10-wk-old hippocampus (M, U) or cerebellum (O, W) of *Npc1*$^{+/+}$ mice, whereas some astrocytes (arrows; N, P) but not microglia (V, X) show immunoreactive PEN2 in *Npc1*$^{-/-}$ hippocampus (N, V) and cerebellum (P, X). Histograms represent PEN2 levels from 3 separate experiments. Abbreviations are same as Fig. 2. Scale bar = 50 μM. *p<0.05, **p<0.01.

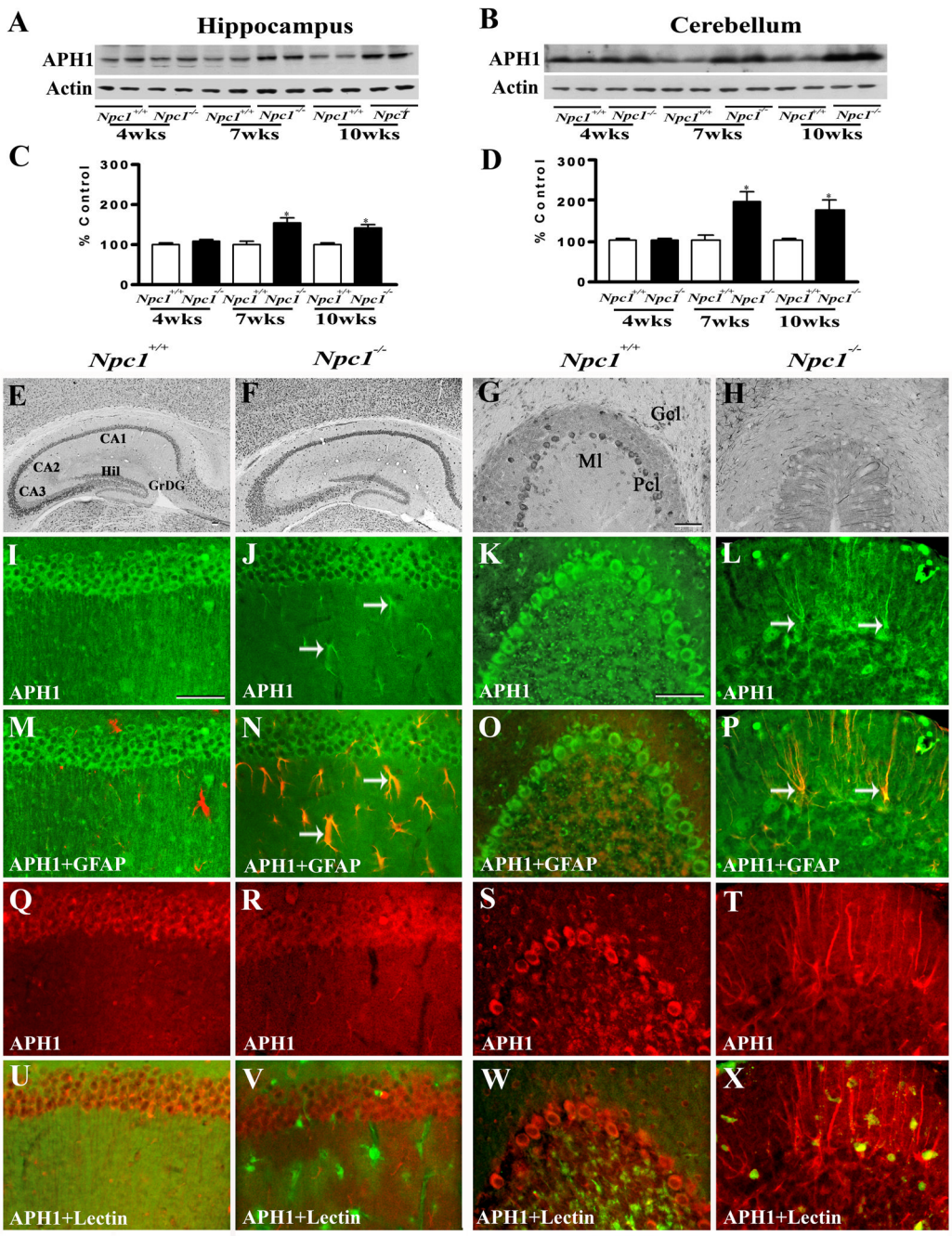

Fig. 7.

A–D; Immunoblots (A, B) and histograms (C, D) showing the level of anterior pharynx defective 1 (APH1) in the hippocampus (A, C) and cerebellum (B, D) of 4-, 7- and 10-week-(wk) old *Npc1*$^{-/-}$ mice compared to controls (*Npc1*$^{+/+}$). E–H; Photomicrographs depicting the loss of APH1-positive neurons in the cerebellum (G, H) but not in the hippocampus (E, F) of 10-wk-old *Npc1*$^{-/-}$ (F, H) mice compared to controls (*Npc1*$^{+/+}$; E, G). I–X; Double labeling showing that immunoreactive APH1 (I–L, Q–T) is not expressed in astrocytes (M, O) or microglia (U, W) in 10-wk-old hippocampus (M, U) or cerebellum (O, W) of *Npc1*$^{+/+}$ mice, whereas a number of reactive astrocytes (arrows; N, P) but not microglia (V, X) exhibit APH1 immunoreactivity in *Npc1*$^{-/-}$ hippocampus (N, V) and cerebellum (P, X).

Histograms represent quantification of APH1 levels from 3 separate experiments. Abbreviations are same as Fig. 2. Scale bar = 50 μM. *p<0.05, **p<0.01.

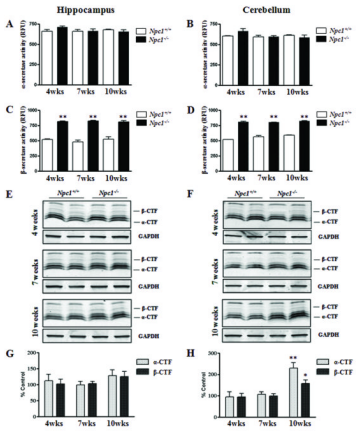

Fig. 8.

A–D; Histograms showing the activity of α- and β-secretases in the hippocampus (A, C) and cerebellum (B, D) of 4-, 7- and 10-week-(wk) old *Npc1*$^{-/-}$ mice compared to age-matched controls (*Npc1*$^{+/+}$). Note that activity of β-secretase (C, D), but not that of α-secretase (A, B), was significantly increased both in the hippocampus and cerebellum of *Npc1*$^{-/-}$mouse brains. E–H; Immunoblots (E, F) and respective histograms (G, H) showing the level of α- and β-CTFs in the hippocampus (E, G) and cerebellum (F, H) of 4-, 7- and 10-week- (wk) old *Npc1*$^{-/-}$ mice. Histograms represent quantification of α-CTF and β-CTF levels from 3 separate experiments. *p<0.05, **p<0.01.